

ROCK HUNTING WITH MARTIAN MACHINE VISION

David Noever and Samantha E. Miller Noever

PeopleTec, Inc., Huntsville, Alabama, USA

david.noever@peopletec.com

ABSTRACT

The Mars Perseverance rover applies computer vision for navigation and hazard avoidance. The challenge to do onboard object recognition highlights the need for low-power, customized training, often including low-contrast backgrounds. We investigate deep learning methods for the classification and detection of Martian rocks. We report greater than 97% accuracy for binary classifications (rock vs. rover). We fine-tune a detector to render geo-located bounding boxes while counting rocks. For these models to run on microcontrollers, we shrink and quantize the neural networks' weights and demonstrate a low-power rock hunter with faster frame rates (1 frame per second) but lower accuracy (37%).

KEYWORDS

Neural Networks, Image Classification, Remote Imagery, Microcontroller

1. INTRODUCTION

The Mars Perseverance rover and its Ingenuity helicopter offer opportunities for the application of computer vision [1-8]. Engineering tasks include obstacle avoidance [8], path planning, and robotic navigation [4-5]. Scientific tasks include rock classification [3,6], object



Figure 1. NASA Perseverance Panorama on Sol 3. The large panorama consists of stitched together frames (142 total) taken using the Mastcam-Z stereo camera.

detection, and elevation mapping. As an extreme example of edge computing, processors with autonomous decision-making make possible rapid mission planning [9] and auto-navigation. Its field-programmable gate arrays (FPGA, Virtex-5) perform maneuver controls for entry, descent, and landing, but receive new firmware to perform mobility visual processing [9]. When processing stereo-imagery at 0.67 frames per second and large 20-megapixel full-color CMOS sensors [9], Perseverance possesses a more robust self-driving capability with hazard avoidance compared to its traditional cycles to drive a meter, then wait while taking and processing a new image.

Previous work applying machine learning to automate computer vision has featured site assessments from orbit [9-10]. From an overhead perspective, these trained algorithms act as rock counters. To overcome data latency and transmission delays, several authors [11-12] have explored deep learning and convolutional neural networks for object recognition. These rock counters [11] require training in complex planetary environments, where color contrast, edge detection, shadows, and textures challenge traditional computer vision applications. In the absence of machine learning, these conventional methodologies include algorithms [13] like Histogram Oriented Gradients (HOG), Scale-Invariant Feature Transform (SIFT), and Support Vector Machine (SVM). Typical accuracies for these approaches range from 60-75% [11] compared to 90+% classifier accuracy with deep learning. The original contributions of the present work include 1) dataset collection and object labeling with Perseverance's camera; 2) an object classifier built to

distinguish rocks vs. rover (parts) with expert-level accuracy (>95%), and 3) a rock detector capable of running state-of-the-art deep learning algorithms (scaled Yolov4) on small edge processors. A simplified concept of operations for modern Martian vision applications shares features with autonomous driving on Earth. If one imagines the main task for self-driving balance safety against autonomous decision-making, then the key tasks include navigation (lane-following, turning, etc.) and hazard avoidance (terrain estimation, rock, and hole recognition). An additional opportunity for planetary rovers not shared with their terrestrial counterparts feature autonomous exploration and geological discovery. We discuss options for robotic autonomy and rock identification. The novel helicopter (Ingenuity) mission further offers scouting alternatives for route selection and rock hunting up to 980 feet per flight [9].

2. METHODS

NASA released their first post-processed panorama on 24 February 2021 [14] from their zoomable, stereo camera called Mastcam-Z [15]. On the third Martian day (Sol 3), the rover team published 142 individual images stitched together to form the 360-degree panorama (Figure 1). After downloading the panorama in PNG format (47 MB), we chipped the 75-megapixel image (16000x4721 pixels) into 1583 sub-images (224x224 pixels, Figure 2). To accommodate transfer learning approaches, we selected this chip size to speed up training for MobileNetV2 classifiers [16] and YOLOv4 scaled [17-18] methods. For all cases, we split the training, validation, and test sets into traditional 70:15:15 ratio of counts.

Classifier. We sorted the images into 3 categories (“other”, “rock”, and “rover”) using human labelers and a python GUI program to separate them into separate folders [19]. The other category includes the Martian sky, soil without rocks, and distant mountains or craters. The rover category includes spacecraft parts as seen by the Mastcam-Z, including wheels and the rover body. A single rock in the image (or multiple) would categorize the chip as a positive case of the rock class. Using transfer learning and a partially pre-trained MobileNetV2 model, we first built a multi-class object recognition model using fine-tuning parameters (epochs=50, batch size =16, learning rate = 0.001). The premise behind transfer learning follows from the empirical observation that feature hierarchies built from large image datasets and different domains provide the core framework for analyzing new unrelated image classes. The benefits for classification include higher accuracy and a lower number of images per class.

Detector. Beyond classification (“Is there a rock or rover somewhere in the image?”), we place bounding boxes and confidence intervals around each Martian rock. Of the original panorama, we chipped out 692 sub-images (416x416 pixels) that included rocks. We bounded each rock (1314) in the images using human labelers and a python GUI program [21] to annotate and format the pixel

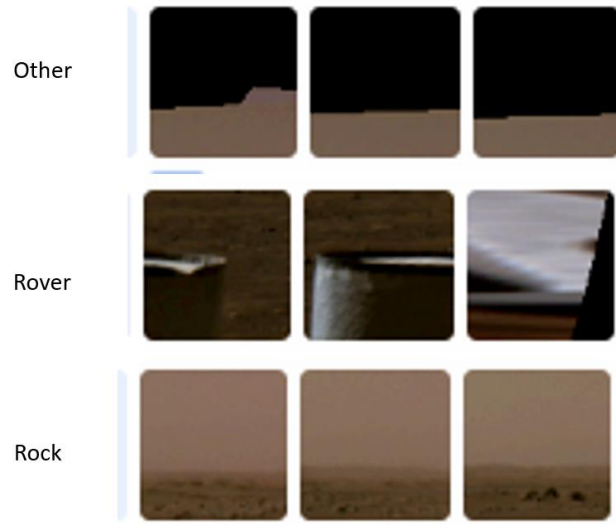


Figure 2 Example panels for multi-class identification

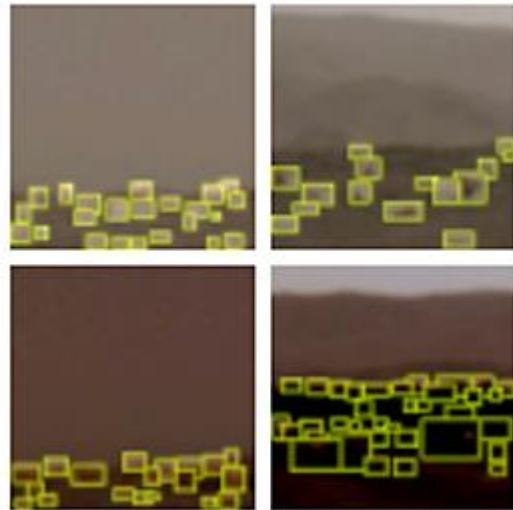


Figure 3. Bounding boxes around rocks in training data

locations in rectangular boxes. Various authors [22] have offered a range of minimum image counts between 100 and 1000 per class, although some few-shot or zero-shot approaches [23] succeed for classification alone with fewer than 10 for uncommon objects. The scaled YoloV4 [17-18] provides a convenient starting point for fine-tuning a custom real-time object detector. In its balance of accuracy and speed, this model approaches the 15-30 frames per second typically regarded as video-quality for real-time in the literature. The model summary includes 235 layers, 52.5 million parameters, and 50.5 million gradients.

3. RESULTS

Figure 4 shows the accuracy and confusion matrix for the basic classifier model. For typical human labelers, other studies have identified a classifier with accuracies about 95-97% as typical of expert-level over time, since without automation assistance human labelers tend to underperform over time for tedious tasks [24]. The size for this fine-tuned MobileNetV2 (14 MB) makes the model optimized to run at 30 frames per second on mobile phone processors. It's worth noting that given the risk acceptance for the Ingenuity helicopter, the Mars 2020 team accepted commercial phone-grade boards (Qualcomm Snapdragon 801). These processors exceed the rover's capabilities by several orders of magnitude but lack radiation hardening (and space legacy) for deep space travel [25].

	Rocks	Rover	Other
Rocks	99.0%	1.0%	0.0%
Rover	5.5%	94.5%	0.0%
Other	0.0%	1.3%	98.8%

Figure 4 Confusion matrix for classifier

On-device Performance	Inference Time (ms)	Peak RAM (K)	ROM Usage (M)	Accuracy
Float 32 unoptimized	1718	957.2	1.60	97.0%
Quantized (int8)	859	297.0	0.59	37.2%

Table 1. Comparison of Image Classifiers Optimized for Microcontrollers

To explore the classifier performance, we ported the trained model to an Arduino Nano 33 BLE Sense device [26]. This low-cost device offers an Arm Cortex-M4 microcontroller running at 64 MHz with 1MB Flash memory and 256 KB of RAM. We deployed the model as an Arduino Sketch using the Edge Impulse platform [27]. Table 1 summarizes the on-device performance modeling for an unoptimized weight model (float32) and quantized (int8). The tradeoff between accuracy, speed, and size favors the float32 weights for accuracy to classify whether a test Martian image contains rocks or rover. Typical post-training gains from quantizing feature 75% smaller models with 200% faster execution. Given the color similarities, shadows, and lack of edge features, the accuracy for this example falls off sharply and would not represent a good deployment selection compared to the float32 version on microcontrollers.

Figure 5 shows a single frame of the rock detector (and counter) using the inference stage of YoloV4 on previously unseen test images. A summary video of rock detection is available online [28]. We constructed the video from multiple stacked images in a slideshow fashion with the bounding boxes placed around each identified rock. Using GPU (Nvidia Quadro M1200), this rock detector processes 40 frames per second (416x416 pixels) and counts the rock density ranging from 0-34 rocks per frame. The bounding box output optionally overlays both the object label and associated confidence intervals (0-1).



Figure 5. Bounding box detector for Mastcam-Z imagery

4. DISCUSSION AND CONCLUSIONS

This research explores the training of a classifier and detector for Martian rock discovery. We demonstrate greater than 97% accuracy for distinguishing rock versus rover from a single large image chipped into

multiple frames and labeled for location (1314 total). We shrink the model with quantized weights and benchmark its performance for frame rate and accuracy on low-cost, low-power microcontrollers. Because of the low-contrast background of the initial panorama, the larger model (float32) outperforms the faster, smaller one. Future work can highlight the application of these trained models to automate the study of rock densities as the rover collects more imagery in different locations, lighting, and viewing angles.

ACKNOWLEDGMENTS

The author would like to thank the PeopleTec Technical Fellows program for encouragement and project assistance.

REFERENCES

- [1] Farley, Kenneth A., Kenneth H. Williford, Kathryn M. Stack, Rohit Bhartia, Al Chen, Manuel de la Torre, Kevin Hand, et al. "Mars 2020 mission overview." *Space Science Reviews* 216, no. 8 (2020): 1-41.
- [2] Zheng, Y. C. (2020). Mars Exploration in 2020. *The Innovation*, 1(2), 100036.
- [3] Stack, Kathryn M., Nathan R. Williams, Fred Calef, Vivian Z. Sun, Kenneth H. Williford, Kenneth A. Farley, Sigurd Eide et al. "Photogeologic map of the Perseverance rover field site in Jezero Crater constructed by the Mars 2020 Science Team." *Space Science Reviews* 216, no. 8 (2020): 1-47.
- [4] Maki, J. N., D. Gruel, C. McKinney, M. A. Ravine, M. Morales, D. Lee, R. Willson et al. "The Mars 2020 engineering cameras and microphone on the Perseverance rover: A next-generation imaging system for Mars exploration." *Space Science Reviews* 216, no. 8 (2020): 1-48.
- [5] Bell, J. F., J. N. Maki, G. L. Mehall, M. A. Ravine, M. A. Caplinger, Z. J. Bailey, S. Brylow, et al. "The Mars 2020 Perseverance rover mast camera zoom (Mastcam-Z) multispectral, stereoscopic imaging investigation." *Space Science Reviews* 217, no. 1 (2021): 1-40.
- [6] Allwood, Abigail C., Joel A. Hurowitz, Benton C. Clark, Luca Cinquini, Scott Davidoff, Robert W. Denise, W. Timothy Elam, et al. "The PIXL Instrument on the Mars 2020 Perseverance Rover." *arXiv preprint arXiv:2103.07001* (2021).
- [7] Boeder, Paul A., and Carlos E. Soares. "Mars 2020: mission, science objectives and build." In *Systems Contamination: Prediction, Control, and Performance 2020*, vol. 11489, p. 1148903. International Society for Optics and Photonics, 2020.
- [8] Abcouwer, Neil, Shreyansh Daftry, Siddarth Venkatraman, Tyler del Sesto, Olivier Toupet, Ravi Lanka, Jialin Song, Yisong Yue, and Masahiro Ono. "Machine Learning-Based Path Planning for Improved Rover Navigation (Pre-Print Version)." *arXiv preprint arXiv:2011.06022* (2020).
- [9] Scannell, Tim, "The technology aboard the Mars rover Perseverance: An inside look", *CIO Magazine*, (2020) <https://www.cio.com/article/3569577/the-technology-aboard-the-mars-rover-perseverance-an-inside-look.html>
- [10] Furlán, Federico, Elsa Rubio, Humberto Sossa, and Víctor Ponce. "CNN-based detectors on planetary environments: a performance evaluation." *Frontiers in Neurorobotics* 14 (2020): 85.
- [11] Wilhelm, Thorsten, Melina Geis, Jens Püttschneider, Timo Sievernich, Tobias Weber, Kay Wohlfarth, and Christian Wöhler. "DoMars16k: A Diverse Dataset for Weakly Supervised Geomorphologic Analysis on Mars." *Remote Sensing* 12, no. 23 (2020): 3981.
- [12] Xing, Yan, and Ziyang Liu. "A Preliminary Study on Intelligent Perception of Extraterrestrial Body Surface Based on Deep Learning and Transfer Learning." In *2020 Chinese Automation Congress (CAC)*, pp. 7533-7537. IEEE, 2020.
- [13] O'Mahony, Niall, Sean Campbell, Anderson Carvalho, Suman Harapanahalli, Gustavo Velasco Hernandez, Lenka Krpalkova, Daniel Riordan, and Joseph Walsh. "Deep learning vs. traditional computer vision." In *Science and Information Conference*, pp. 128-144. Springer, Cham, 2019.

- [14] NASA, "Mastcam-Z's First 360-Degree Panorama", (2021), online versions https://www.nasa.gov/sites/default/files/thumbnails/image/pia2464-mastcam-zs_first_360-degree_panorama2.jpg and <https://www.nasa.gov/image-feature/jpl/mastcam-z-s-first-360-degree-panorama>
- [15] Bell, J. F., J. N. Maki, G. L. Mehall, M. A. Ravine, M. A. Caplinger, Z. J. Bailey, S. Brylow, et al. "The Mars 2020 perseverance rover mast camera zoom (Mastcam-Z) multispectral, stereoscopic imaging investigation." *Space Science Reviews* 217, no. 1 (2021): 1-40.
- [16] Sandler, Mark, Andrew Howard, Menglong Zhu, Andrey Zhmoginov, and Liang-Chieh Chen. "Mobilenetv2: Inverted residuals and linear bottlenecks." In *Proceedings of the IEEE conference on computer vision and pattern recognition*, pp. 4510-4520. 2018.
- [17] Bochkovskiy, Alexey, Chien-Yao Wang, and Hong-Yuan Mark Liao. "Yolov4: Optimal speed and accuracy of object detection." *arXiv preprint arXiv:2004.10934* (2020).
- [18] Wang, Chien-Yao, Alexey Bochkovskiy, and Hong-Yuan Mark Liao. "Scaled-YOLOv4: Scaling Cross Stage Partial Network." *arXiv preprint arXiv:2011.08036* (2020).
- [19] Baumgartner, Christian "image-sorter2", (2020), <https://github.com/Nestak2/image-sorter2>
- [20] Cai, Han, Chuang Gan, Ligeng Zhu, and Song Han. "Tiny transfer learning: Towards memory-efficient on-device learning." *arXiv preprint arXiv:2007.11622* (2020).
- [21] Tzutalin. LabelImg. Git code (2015). <https://github.com/tzutalin/labelImg>
- [22] Patel, Srujan, Naeem Patel, Siddhesh Deshpande, and Amroz Siddiqui. "Ship Intrusion Detection using Custom Object Detection System with YOLO Algorithm." (2021).
- [23] Romera-Paredes, Bernardino, and Philip Torr. "An embarrassingly simple approach to zero-shot learning." In *International conference on machine learning*, pp. 2152-2161. PMLR, 2015.
- [24] Noever, David, and Samantha E. Miller Noever. "Overhead MNIST: A benchmark satellite dataset." *arXiv preprint arXiv:2102.04266* (2021).
- [25] NASA Mars Rover Brains, (2020), <https://mars.nasa.gov/mars2020/spacecraft/rover/brains/>
- [26] Arduino Tiny ML Kit, (2020), <https://store.arduino.cc/usa/tiny-machine-learning-kit>
- [27] Edge Impulse, (2020), <https://docs.edgeimpulse.com/docs>
- [28] Mars Rock Detector Video, <https://deeperbrain.com/demo/rocks.html>